Reversible oxygen doping of conjugated polymer and its dedoping studied by Mott-Schottky analysis

Oleg V. Kozlov[a] and Sergey A. Zapunidi[a]

[a]: International Laser Center and Faculty of Physics, M.V. Lomonosov Moscow State University, Leninskie Gory, 1, Moscow RU-119991, Russia

Corresponding Author:

Oleg V. Kozlov

International Laser Center, M.V. Lomonosov Moscow State University, Leninskie Gory, 1, Moscow RU-119991, Russia

PHONE +7(495)9392228
FAX +7(495)9393113

Email ov.kozlov@physics.msu.ru

Abstract

One of the important factors influencing on organic solar cells efficiency is doping of the polymer by atmospheric oxygen. It's known already that the doping may be partially reversed by annealing of the device, but the phenomenon is not well-studied yet. In this paper we studied processes of doping and dedoping of conjugated polymers, using well-known poly(3-hexylthiophene) (P3HT) and derivative of new low-bandgap polymer poly(3,4-ethylenedioxyselenophene) (PEDOS-C_{12}), by impedance spectroscopy.

Possibility of dedoping under annealing was examined for both of the polymers. Influence of annealing atmosphere and sample preparation conditions on dedoping process were studied along with dynamics of self-doping and dedoping processes and influence of light on self-doping dynamics. Dedoping dynamics in inert atmosphere turn out to be biexponential.

1 Introduction

One of the main application areas for conjugated polymers is organic electronics, in particular, organic photovoltaics. Organic solar cells have some attractive advantages in comparison with traditional silicon solar cells like flexibility, semitransparency, ease of manufacturing, etc. But organic solar cells are not widely used today because of their relatively low efficiency (below 10% [1]) and low stability (the efficiency of P3HT-based solar cell decreases dramatically in a few days [2-4]).

One of the crucial factors influencing on organic solar cells efficiency is doping of the polymer. It's well-known that some polymers (widely used P3HT for example) are inclined to self-doping by atmospheric oxygen in contact with air [5-8]. Doping of the active layer of organic solar cell may lead to decreased short-circuit current [9] and fill factor because of reduced charge generation region [10, 11]. Thus, organic solar cell degradation with time may be also connected with gradual oxygen doping of the polymer [12].

Minimization of manufacturing cost of organic solar cells is desirable in industrial manufacturing. So most of the steps including solution stirring, film casting and device posttreatment better be performed under ambient conditions. Hence, studying and describing the processes of polymer interaction with atmospheric oxygen and finding ways to prevent or reverse polymer's oxygen doping are really important.

Recently a number of papers devoted to processes and mechanisms of interaction between P3HT and oxygen were published [12-15]. In [14, 15] two possible mechanisms (reversible and irreversible) of polymer-oxygen interaction were suggested. Schematic representation of these mechanisms is shown on Fig. 1. One of the channels (irreversible

channel, red color on Fig. 1) is a chemical oxidation of the polymer and it only occurs under illumination. The other channel (reversible, green color on Fig. 1) is related to formation of weak charge-transfer complex (CTC) between polymer and oxygen proposed by Abdou et al. [16], and it occurs both in dark and under illumination. Since bonding energy of the CTC is relatively weak it can dissociate under influence of high temperatures, and in [12-15] possibility of dedoping of P3HT thin film under annealing in vacuum or in inert atmosphere was proved experimentally. But this problem isn't fully studied yet. First of all, possibility of dedoping was shown qualitatively, but there are no quantitative evaluations of dedoping level yet. It remains unclear if the dedoping effect under annealing is common phenomena or it only takes place for P3HT. Further, it was shown that polymer's solution can be doped with oxygen [16], but it's unclear if this process is reversible too. Furthermore the doping and dedoping processes dynamics and environment influence on dedoping process are still unexamined. So generalization of doping and dedoping processes with quantitative evaluations should be performed.

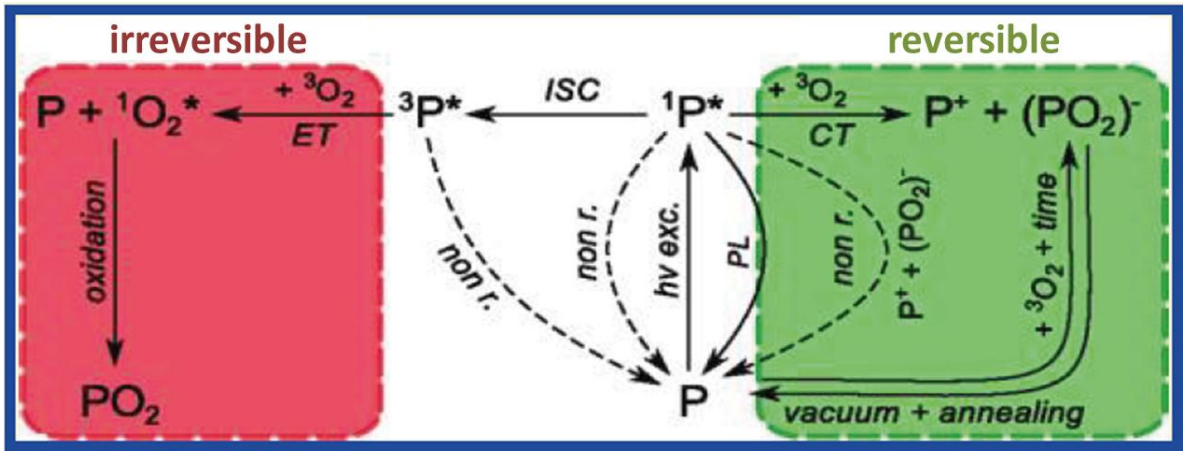

Fig. 1 Schematic representation of reversible and irreversible interactions between polymer and oxygen [15]

Direct measurements of doping concentration in a polymer film may be convenient to study doping and dedoping processes. One of the possibilities to measure doping concentration is based on Schottky barrier formation when a p-doped semiconductor contacts with metal with lower workfunction. Inverse square of the barrier's capacitance is a linear function of bias voltage (it also called Mott-Schottky behavior) [17, 18]:

$$\frac{1}{C^2} = \frac{2(V_s - V)}{S^2 q N_a \varepsilon \varepsilon_0}, \quad (1)$$

Here C is the barrier capacitance, V_s is Schottky barrier height, V is bias voltage, S is contact's area, q is elementary charge, Na is doping concentration, ε is relative permittivity of the active layer and ε_0 is vacuum permittivity. Schottky barrier's height (also called as flat-band voltage) is determined by difference between Fermi levels of the polymer and the electrode.

The width of the depletion layer can be calculated as [17]:

$$W = \sqrt{\frac{2\varepsilon\varepsilon_0(V_s - V)}{qN_a}}, \quad (2)$$

Thus, one of the simple ways to estimate doping concentration of polymer's film is a device construction, where Schottky barrier capacitance can be measured [9].

2 Sample preparation and experimental

To study self-doping and dedoping processes of conjugated polymers samples based on widely used polymer P3HT (Fig. 2, a) and new promising low bad-gap polymer PEDOS-C_{12} [19] (Fig. 2, b) were made.

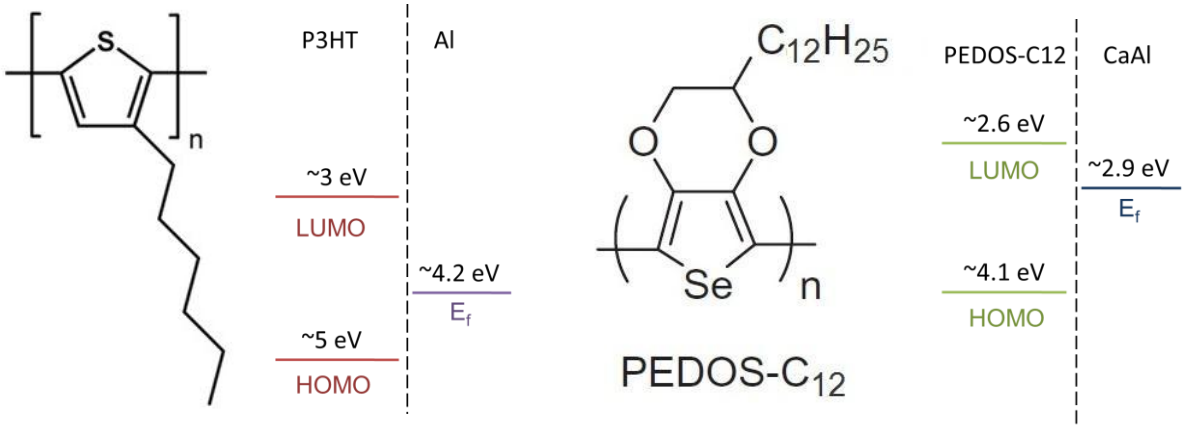

a) b)

Fig. 2 Structural formulas and energy level diagrams for P3HT (a) and PEDOS-C_{12} (b)

Dichlorobenzene solution of polymers was prepared at concentrations of 30 g/l for P3HT and 10 g/l for PEDOS-C_{12}. Solutions were stirred on a magnetic stirrer for at least 12 hours at 75°C. Diodes were fabricated on ITO-covered substrates. Thin layer of PEDOT:PSS was spin-casted at 3000 rpm for 2 min on the substrate from aqueous solution first. Then substrates was annealed at 150°C for 15 min in air to remove any remaining water of the PEDOT:PSS film. The polymer film was then spin-casted from solution at 1000 rpm for 2 min. The whole sample preparation process was performed in air and self-doping of the polymer solution was occurring. One control sample based on P3HT was prepared in an argon glovebox.

After polymer film casting the second electrode was thermally evaporated through a mask. The evaporation was done at 7×10^{-6} mbar pressure. Aluminum was chosen as an electrode for P3HT-based samples as it is well-known that Schottky barrier forms on the P3HT-Al interface [13, 20]. For PEDOS-C_{12}-based sample the second electrode was made of CaAl since its Fermi level is lower than the polymer's HOMO (Fig. 2, b). Schematic picture of the sample is shown on Fig. 3. Thicknesses of the films were estimated using conventional AFM profiling as 220±20 nm for P3HT-based diodes and 30±20 nm for PEDOS-C_{12}-based one.

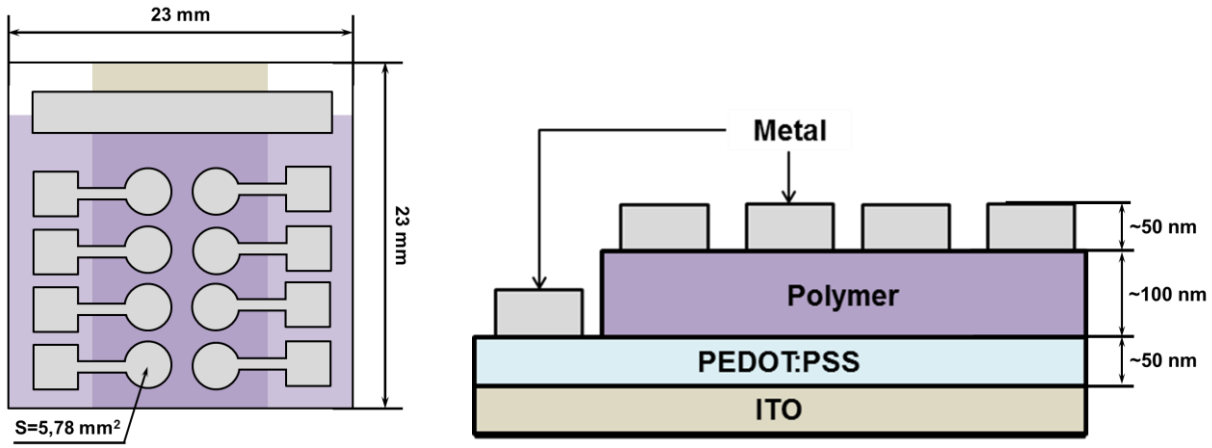

Top view Side view

Fig. 3 Schematic image of the sample

The samples were measured using Elins Z-1000P impedance analyzer. To estimate realistic concentration of acceptor impurities a proper frequency of AC voltage should be chosen. This frequency may be chosen from capacitance-frequency analysis. Fig. 4 shows frequency dependent capacitance for a P3HT-based diode. As clear from the figure, capacitance doesn't saturate on presented frequency scale. However, it increases rapidly up to 10 kHz and grows insignificantly further. Consequently, the frequency should be as low as possible in range below 10 kHz. In order to obtain acceptable signal-to-noise ratio, modulation frequency of 500 Hz was chosen. Measurements were performed under different bias voltages ranging from -600 to 1750 mV with amplitude of 25 mV.

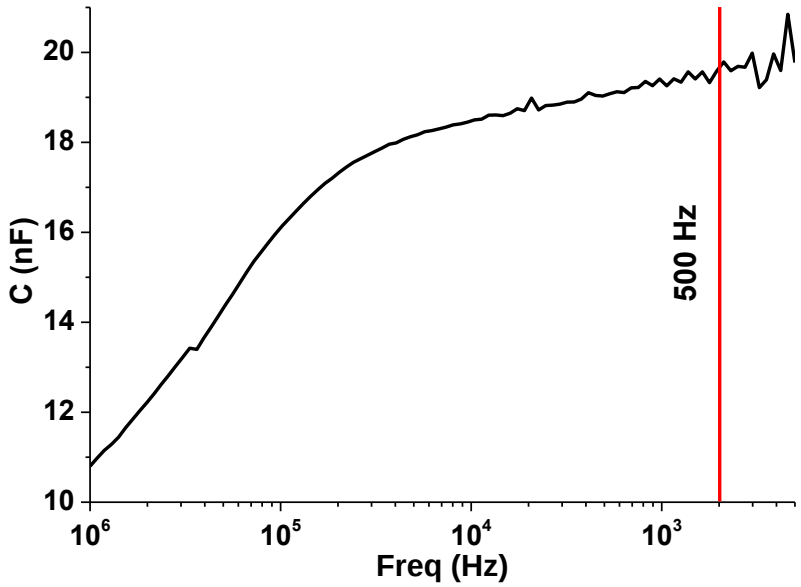

Fig. 4 Capacitance vs. frequency for a P3HT-based sample

The samples were measured right after preparation. Then the samples were annealed for 10 min at 140°C. Annealing was performed either in the argon glovebox (<100 ppm H_2O, <100

ppm O_2) or under ambient conditions. After first annealing the samples were kept in atmospheric air for 5 days and then second annealing was performed. So, experiment consists of several steps (manufacturing of the sample, first annealing either in glovebox or in air, storing in air and second annealing), and doping concentration was measured after each step.

For self-doping dynamics measurements an annealed sample was kept in air either under ambient light or in dark. Doping concentration was measured every day. For dedoping dynamics studies the samples were annealed at 100°C and the measurements were performed directly during annealing process.

3 Experimental results

All samples showed Schottky-diode-like behavior. The linear part of Mott-Schottky curve was fitted using (1) in assumption of pixel square S=5.78 mm^2 and dielectric coefficient ε=3 [21, 22].

3.1 Influence of annealing on doping concentration

First of all, it is necessary to make sure that annealing doesn't affect undoped sample, so a control experiment was performed. Influence of annealing on the glovebox-made control P3HT-based sample was measured in this experiment. The sample was annealed in glovebox, and after annealing the sample was stored in atmospheric air for 5 days and then it was annealed again. First annealing shouldn't change doping concentration in the sample. Then doping concentration should increase during air storing and then decrease to initial value after second annealing. The experiment scheme for this sample is shown on Fig. 5 a) and Mott-Schottky curves are shown on Fig. 5 b). As follows from Fig. 5 after first annealing doping concentration barely changes and second annealing almost restore the doping concentration to its initial value as we expected.

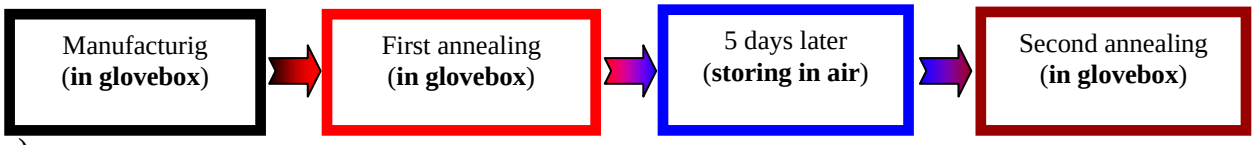

a)

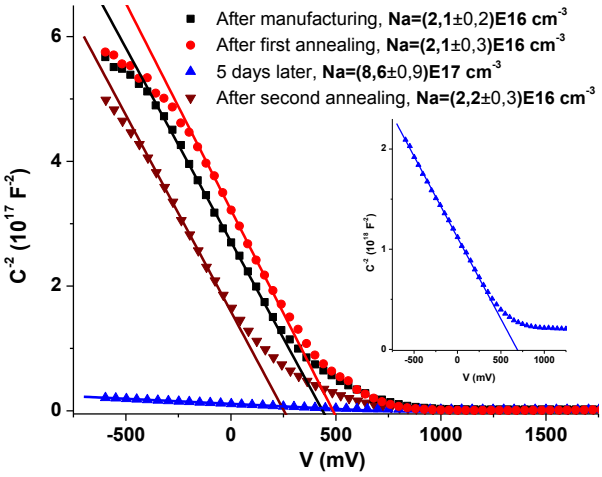

b)

Fig. 5 Experiment scheme (a) and Mott-Schottky curves (b) for the control glovebox-made P3HT sample

The similar experiment was performed for the air-made P3HT sample to verify possibility of dedoping of the polymer doped during solution stirring. Since the sample was exposed to self-doping during manufacturing its initial doping concentration was expected to be higher than in the control sample. Also rough equalizing of doping concentration in these samples after annealing was expected. The experiment scheme for this sample is shown on Fig. 6 a).

Fig. 6 b) and c) shows Mott-Schottky curves for this sample. As follows from Fig. 6 b), first annealing decreased the doping concentration by ~4E-16 cm^{-3}. In contrast, annealing of control glovebox-made sample did not lead to its dedoping (see Fig. 5 b). The only difference between air-made and control samples was that in case of air-made sample the solution of the polymer was stirred in ambient air for more than 12 hours, and the thin film was spin-casted under atmospheric conditions no longer than 5 minutes before it was placed in argon glovebox. Increasing of doping concentration during film casting should be as low as ~1E-15 cm^{-3} (see Fig. 10). Hence, one can conclude that most of oxygen was collected by polymer in its dissolved state, and removed from its solid state. Consequently, doping of polymer's solution is reversible.

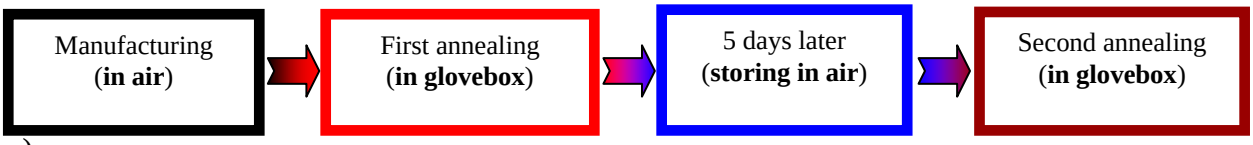

a)

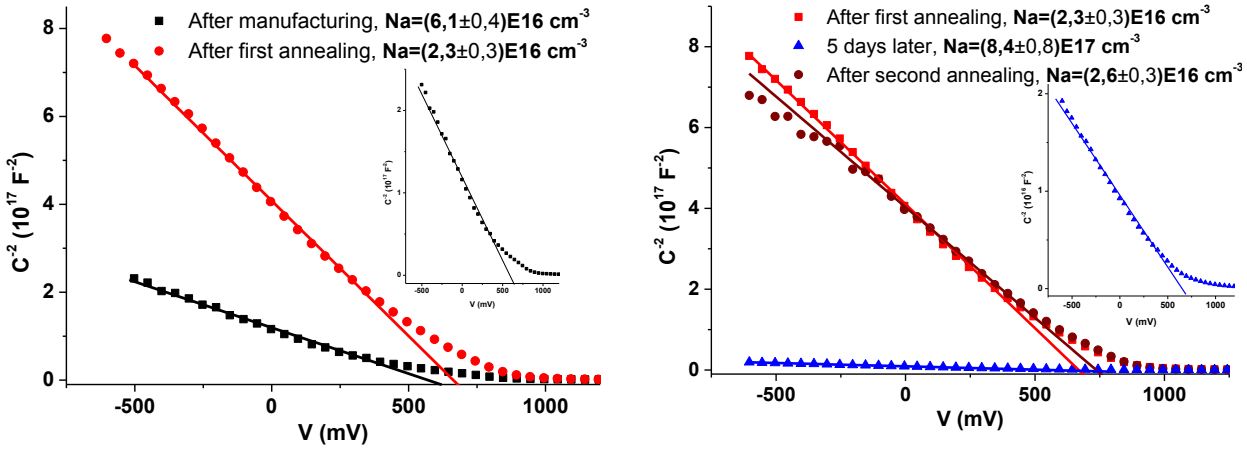

b) c)

Fig. 6 Experiment scheme (a) and Mott-Schottky curves after first (b) and second (c) annealing for the air-made P3HT sample

The next P3HT-based sample was annealed under ambient conditions to examine influence of oxygen presence during annealing on the sample. After second annealing the sample was annealed once again in the glovebox. The experiment scheme is shown on Fig. 7, a).

Fig. 7 b), c) show plots illustrating annealing influence on the sample. It's clear that along with a decrease of the doping concentration after air-performed annealing the plot's shape changed also. The Mott-Schottky plot bended and a straight part of plot became barely determined, so doping concentrations values for this sample are only evaluative. It should be noted also, that additional annealing in inert atmosphere is not able to restore the plot's shape in its initial form. So it can be concluded that air annealing leads to irreversible qualitative changes in the sample, probably related to the polymer-oxygen chemical interaction.

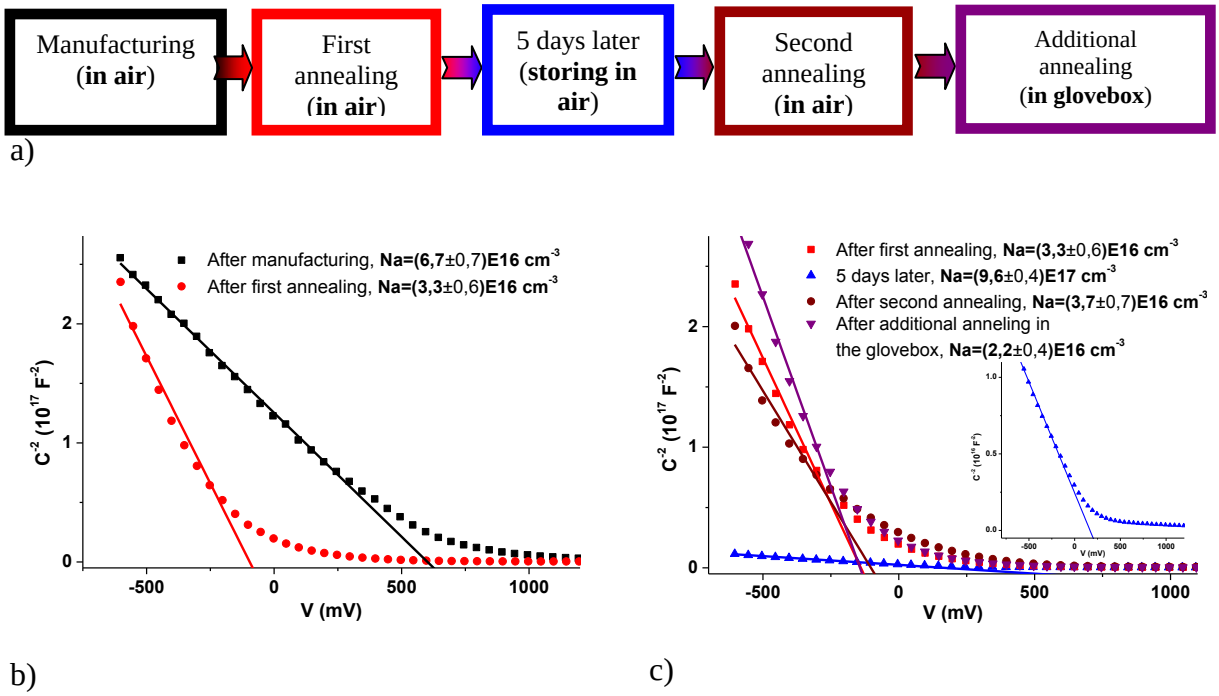

Fig. 7 Experiment scheme (a) and Mott-Schottky curves after first (b) and further (c) annealing in air for the air-made P3HT sample

Similar experiments were performed for the PEDOS-C_{12} based sample made in air. The experiment scheme is shown on Fig. 8 a). Since the highest possible doping concentration of the polymer depends on its energy levels [12], we expected that doping concentration in PEDOS-C_{12} would be higher than in P3HT because of its higher HOMO (Fig. 2).

Fig. 8 b), c) show Mott-Schottky plots for this sample. As follows from these figures, annealing in inert atmosphere is capable of dedoping of this sample and also it can return the sample stored in the air for 5 days to its initial state.

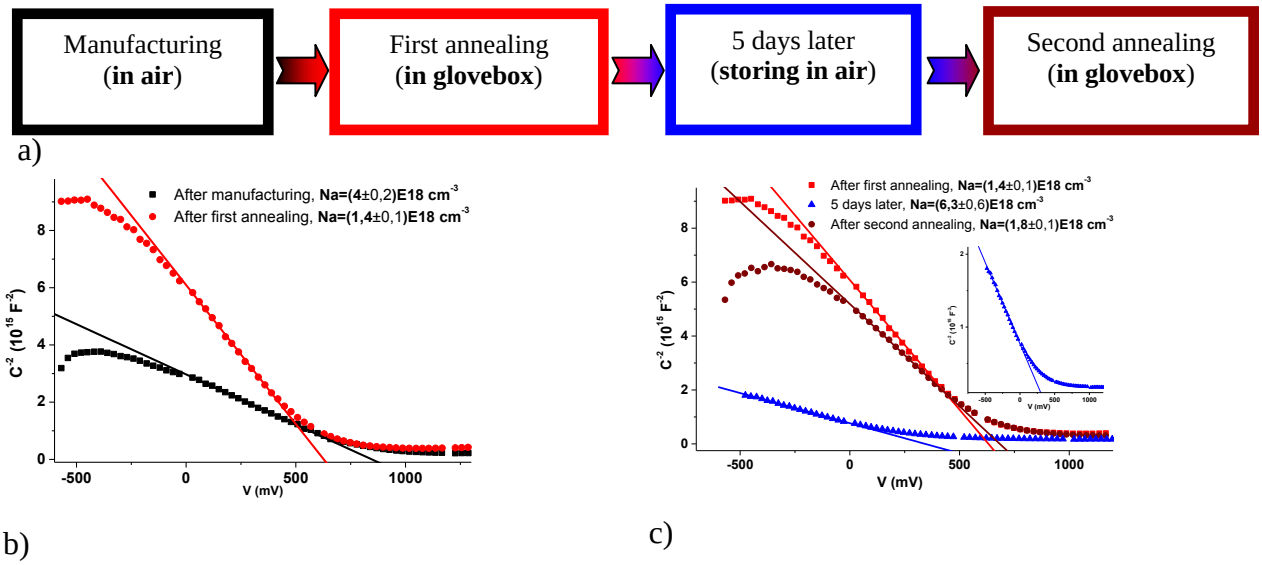

Fig. 8 Experiment scheme (a) and Mott-Schottky curves after first (b) and second (c) annealing for the PEDOS-C_{12}-based sample

One can notice that Mott-Schottky plots of PEDOC-C_{12}-based diodes reach saturation at low-reverse voltages (~-500 mV), which is explained by small thickness of PEDOC-C_{12} layer (about 20 nm). Indeed, in accordance to (2) depletion layer width can easily exceed the film's thickness.

3.2 Analysis of annealing influence

Doping concentrations and flat-band voltages for all samples are given in Table 1. Doping concentrations for the P3HT-based samples are in good agreement with previously published data [7, 12, 18, 20, 23, 24]. We believe that glovebox annealing is able to remove all collected oxygen from air-made sample, because the doping concentration of the air-made sample has reduced to the level of doping concentration of glovebox-made one. Also the doping concentrations of all samples after second annealing in inert atmosphere reduced to the doping level after first annealing, so an increase of doping concentration in the polymer film during storing in atmospheric air is a fully reversible process. The only irreversible process occurs only during annealing in air.

Doping concentration, 10^{16} cm^{-3} (Flat-band voltage, V)	**After manufacturing**	**After first annealing**	**5 days later**	**After second annealing**
P3HT №1 (control)	2,1±0,2 (440±70)	2,1±0,3 (480±70)	86±9 (700±90)	2,2±0,3 (250±60)
P3HT №2 (glovebox-annealed)	6,1±0,4 (600±80)	2,3±0,3 (640±80)	84±8 (650±90)	2,6±0,3 (670±80)
P3HT №3 (air-annealed)	6,7±0,7 (600±80)	3,3±0,6 (-100±70)	96±4 (170±60)	3,7±0,7 (-80±40) (annealing in air) 2,2±0,4 (-120±50) (annealing in glovebox)
PEDOS-C_{12}	400±24 (850±120)	143±13 (630±90)	625±61 (350±60)	184±10 (680±100)

Table 1 Doping concentrations and flat-band voltages for all samples

As clear from Table 1, annealing process and interaction with oxygen influence not only doping concentration within the device, but its flat-band voltage too. Unfortunately, changing of flat-band voltage seems to be unsystematic. Furthermore, from detailed analysis of plots for all samples (Fig. 5-Fig. 7) one can see that all measured Mott-Schottky curves approach their constant value smoothly, and the bend ends approximately at 750 mV, which corresponds to

difference between P3HT HOMO level and aluminum Fermi energy. This bend is expressed mostly for air-annealed sample, which in fact does not show linear part at all.

Such behavior of Mott-Schottky plots may be related to alteration of polymer structure under influence of oxygen. Oxidizing of polymer unit in the polymer chain creates defect level within the bandgap [25], making the effective Fermi level of the polymer film inhomogeneously broadened. As a result, a lot of Schottky barriers with distribution of heights appears. This distribution leads to bending of Mott-Schottky plot and shifting of effective flat-band voltage (see Fig. 9).

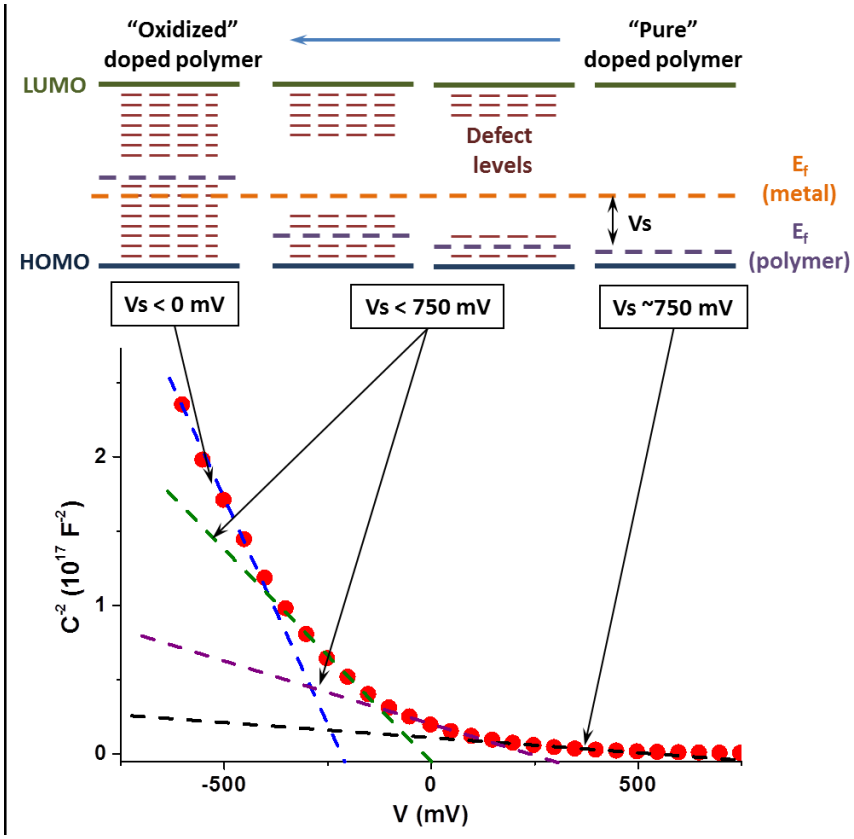

Fig. 9 Schematic representation of Mott-Schottky plot bending

Also one can notice that doping concentration of the PEDOS-C_{12}-based sample is nearly two orders of magnitude higher that the concentration of P3HT-based samples, which agrees with assumption of dependence of doping concentration on HOMO level of the polymer. But after 5 days of contact with atmospheric air doping concentration in the PEDOS-C_{12}-based sample increases only 4 times, while in the P3HT-based sample the doping concentration increases 40 times. It may be caused by the difference of electrode materials in these samples, because it is known that oxygen can diffuse through aluminum electrode into the film easily [26, 27].

A P3HT-based sample with CaAl electrodes was made to confirm this assumption (Mott-Schottky plots for this sample are not presented). Doping concentration in this sample increases

from 2,2E16 cm^{-3} to 9E16 cm^{-3} during 5 days in air storage. So, indeed, the difference in electrode's material may influence the doping speed.

3.3 Dynamics of doping of the conjugated polymer in contact with atmospheric air

Increasing of doping concentration of thin polymer film with time can be described with a following model. Let us suppose that the oxygen concentration in the thin film of the polymer is constant because of rather high diffusion coefficient of oxygen in P3HT film (D_{O2}~10^{-7} cm^2s^{-1} [28]) and small thickness of the film (~200 nm). So the thin films are equilibrated with oxygen within time scale of milliseconds. Then let each molecule of polymer bond with oxygen with probability of P(I) dependent on light intensity I. Then, the number of undoped polymer in the film is described as ($N_P - N_a$), where N_P is a total concentration of polymer molecules in the film and N_a is doping concentration. So increase of polymer doping in the film by the time dt will be:

$$dN_a = P(I) * N_O * (N_P - N_a) * dt, \tag{3}$$

where N_O is number of oxygen molecules in the film. So the doping concentration in the film is in exponential dependence with time:

$$N_a(t) = N_P - (N_P - N_a^0)e^{-A(I)*t}, \tag{4}$$

where N_a^0 is initial doping concentration and $A(I) = P(I) * N_O$.

Dynamics of doping of the P3HT film is shown on Fig. 10. As follows from the figure, time dependence of doping concentration is linear in case of storing the film both in dark and under ambient room light. So one can conclude that saturation time is much longer than the time of observation (more than two weeks). Also as follows from Fig. 10 the slope of dependence in case of storing film under ambient light is steeper than in case of storing in dark, so self-doping velocity depends on irradiation light intensity.

Since doping concentration is far from saturation the dynamics were fitted with linear part of (4), i.e. with

$$N_a(t) = N_a^0 + V(I) * t, \tag{5}$$

where $V(I) = (N_P - N_a^0) * A(I)$ is a linear velocity of doping. Fit parameters as well as fit curves are shown on Fig. 10.

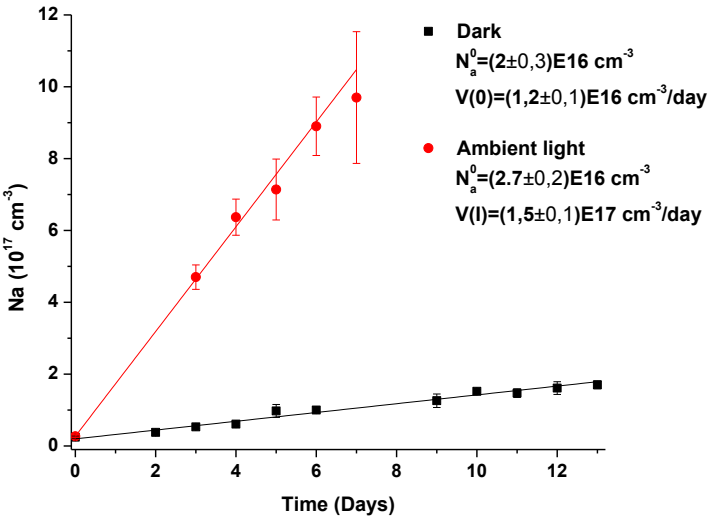

Fig. 10 Time dependence of doping concentration of P3HT film in contact with atmospheric air

3.4 Dynamics of dedoping of the polymer film under annealing

Dynamics of dedoping of the polymer film during annealing was measured for P3HT-based sample in glovebox (Fig. 11). As follows from the figure, dynamics curve shows double exponential behavior, which means that two qualitative different channels of dedoping exist. The dedoping curve was fitted with biexponential decay function, and the fit parameters are given in Table 2. As one can see from the table there are two different timescales of dedoping process – "fast" and "slow". We can't explain this behavior yet, but one of the possible explanations is a difference between dedoping processes in crystalline and amorphous forms of P3HT. Indeed, the annealing temperature approximately equals the P3HT glass transition temperature [29], which implies presence of both crystalline and amorphous forms within the polymer film.

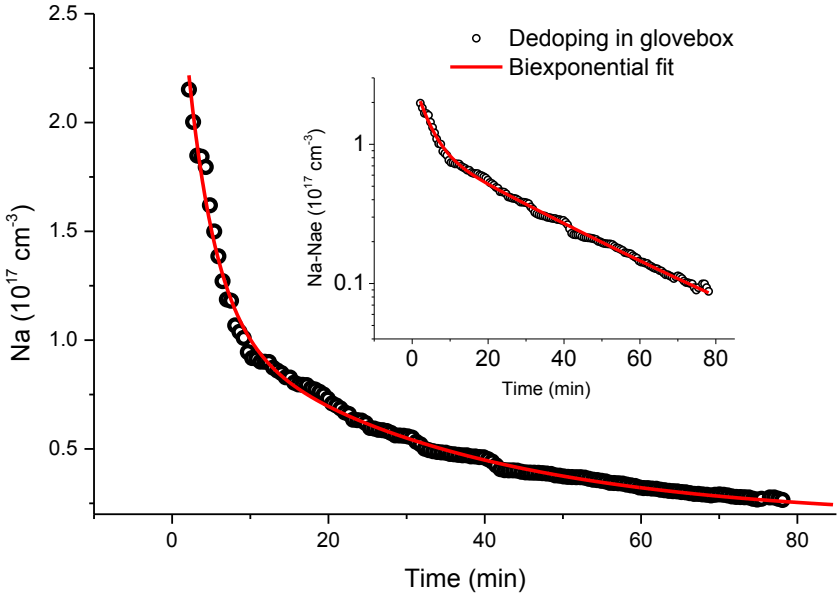

Fig. 11 Dynamics of dedoping of P3HT-based sample in glovebox (log scale in the inset)

Fit function	y_0, 10^{16} cm^{-3}	A_1, 10^{16} cm^{-3}	t_1, minutes	A_2, 10^{16} cm^{-3}	t_2, minutes
$y=y_0+A_1e^{-x/t_1}+ +A_2e^{-x/t_2}$	3,4±0,1	2,9±0,1	7,4±0,2	2,2±0,1	40±2

Table 2 Fit parameters for dynamics of dedoping of P3HT-based sample

Dependence of flat-band voltage of the device on doping concentration during annealing in the glovebox is shown in Fig. 12. As follows from the figure, flat-band voltage of the device increases first, achieving saturated value of approximately 750 mV. Such behavior can be explained with well-known mechanism related to dependence of the semiconductor's Fermi level on doping concentration – higher doping concentration moves the Fermi level toward valence band of the semiconductor. According to this mechanism, the flat-band voltage should increase with increasing of doping concentration toward some saturated value, which is determined by difference between Fermi level of metal electrode and HOMO of the polymer [30]. Indeed, the difference between P3HT HOMO and Fermi energy of aluminum is 0.8 eV (see Fig. 2), which means that measured result is in a good agreement with calculated one. Besides, oxygen doping concentration at which the Fermi level of the polymer lowers down to its HOMO level was estimated as ~7E16 cm^{-3}.

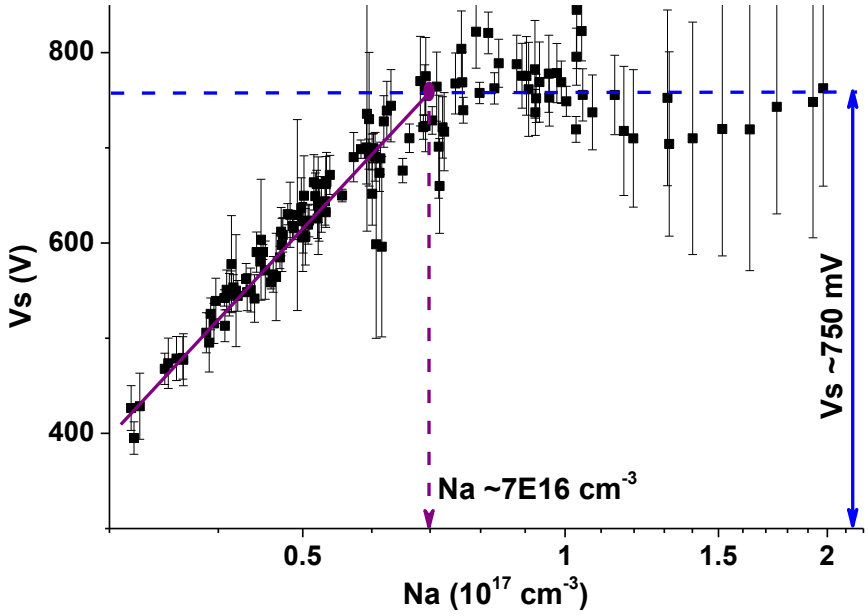

Fig. 12 Flat-band voltage dependence on doping concentration in case of glovebox annealing

4 Conclusion

Using P3HT and PEDOS-C_{12} as examples, it was shown that conjugated polymers are inclined to self-doping in contact with air both in film and in solution. Doping level may depend on the HOMO level of the polymer, and doping velocity depends on electrode material. Also it was shown that doping concentration can be reduced by annealing in glovebox, and doping

concentration of air-made samples can be reduced to the level of glovebox-made sample. In other words, the oxygen doping level of a sample made in air and annealed in glovebox is equivalent to the doping level of a sample made in glovebox. So annealing is simple and effective way to control the doping level of conjugated polymer. However, annealing in air leads to irreversible oxidizing of the polymer, making its effective Fermi level inhomogeneously broadened.

Also linear behavior of time dependence of doping concentration of the polymer either in dark or under illumination was demonstrated. Doping concentration didn't come to saturation during experiment, so saturation time is much more than two weeks. Also it was shown that self-doping velocity depends strongly on irradiating light intensity.

Dedoping process was shown to have double exponential behavior. We assume that the presence of two exponents is related to presence of two forms of polymer in the sample (amorphous and crystalline) and each of them has independent dedoping channel.

Oxygen doping concentration at which the Fermi level of the polymer lowers down to its HOMO level, which leads to saturation of device's flat-band voltage, was estimated as ~7E16 cm^{-3}.

Acknowledgements

We would like to thank Michael Bendikov (Department of Organic Chemistry, Weizmann Institute of Science, Israel) for providing the PEDOS-C_{12} polymer.

References

[1] M.A. Green, K. Emery, Y. Hishikawa, W. Warta, E.D. Dunlop, Solar cell efficiency tables (version 39), Progress in Photovoltaics: Research and Applications, 20 (2012) 12-20.
[2] M.D. Wang, F.Y. Xie, J. Du, Q. Tang, S.Z. Zheng, Q. Miao, J. Chen, N. Zhao, J.B. Xu, Degradation mechanism of organic solar cells with aluminum cathode, Solar Energy Materials and Solar Cells, 95 (2011) 3303-3310.
[3] A. Moujoud, S.H. Oh, J.J. Hye, H.J. Kim, Improvement in stability of poly(3-hexylthiophene-2,5-diyl)/6,6-phenyl-C61-butyric acid methyl ester bulk heterojunction solar cell by using UV light irradiation, Solar Energy Materials and Solar Cells, 95 (2011) 1037-1041.
[4] B. Remi De, J. Leroy, M. Firon, C. Sentein, Accelerated lifetime measurements of P3HT:PCBM solar cells, Synth. Met., 156 (2006) 510-513.
[5] B. Van Der Zanden, A. Goossens, Oxygen Doping of Tio2/Poly(Phenylene-Vinylene) Bilayer Solar Cells, Journal of Applied Physics, 94 (2003) 6959-6965.
[6] M. Glatthaar, M. Riede, N. Keegan, K. Sylvester-Hvid, B. Zimmermann, M. Niggemann, A. Hinsch, A. Gombert, Efficiency limiting factors of organic bulk heterojunction solar cells identified by electrical impedance spectroscopy, Solar Energy Materials and Solar Cells, 91 (2007) 390-393.

[7] G. Garcia-Belmonte, A. Munar, E.M. Barea, J. Bisquert, I. Ugarte, R. Pacios, Charge carrier mobility and lifetime of organic bulk heterojunctions analyzed by impedance spectroscopy, Org. Electron., 9 (2008) 847-851.
[8] S. Hoshino, M. Yoshida, S. Uemura, T. Kodzasa, N. Takada, T. Kamata, K. Yase, Influence of Moisture on Device Characteristics of Polythiophene-Based Field-Effect Transistors, J. Appl. Phys., 95 (2004) 5088-5093.
[9] A. Guerrero, P.P. Boix, L.F. Marchesi, T. Ripolles-Sanchis, E.C. Pereira, G. Garcia-Belmonte, Oxygen doping-induced photogeneration loss in P3HT:PCBM solar cells, Solar Energy Materials and Solar Cells, 100 (2012) 185-191.
[10] V.A. Trukhanov, V.V. Bruevich, D.Y. Paraschuk, Effect of doping on performance of organic solar cells, Phys. Rev. B, 84 (2011) 205318.
[11] J. Schafferhans, A. Baumann, A. Wagenpfahl, C. Deibel, V. Dyakonov, Oxygen doping of P3HT:PCBM blends: Influence on trap states, charge carrier mobility and solar cell performance, Org. Electron., 11 (2010) 1693-1700.
[12] A. Seemann, T. Sauermann, C. Lungenschmied, O. Armbruster, S. Bauer, H.-J. Egelhaaf, J. Hauch, Reversible and irreversible degradation of organic solar cell performance by oxygen, Solar Energy, 85 (2011) 1238–1249.
[13] M. Glatthaar, N. Mingirulli, B. Zimmermann, T. Ziegler, R. Kern, M. Niggemann, A. Hinsch, A. Gombert, Impedance spectroscopy on organic bulk-heterojunction solar cells, Physica Status Solidi a-Applications and Materials Science, 202 (2005) R125-R127.
[14] H. Hintz, H. Peisert, H.-J. Egelhaaf, T. Chasse, Reversible and Irreversible Light-Induced p-Doping of P3HT by Oxygen Studied by Photoelectron Spectroscopy (XPS/UPS), J. Phys. Chem. C, 115 (2011) 13373–13376.
[15] A. Sperich, H. Kraus, C. Deibel, H. Blok, J. Schmidt, V. Dyakonov, Reversible and Irreversible Interactions of Poly(3-hexylthiophene) with Oxygen Studied by Spin-Sensitive Methods, J. Phys. Chem. B, 115 (2011) 13513-13518.
[16] M.S.A. Abdou, F.P. Orfino, Y. Son, S. Holdcroft, Interaction of Oxygen With Conjugated Polymers: Charge Transfer Complex Formation With Poly(3-Alkylthiophenes), Journal of the American Chemical Society, 119 (1997) 4518-4524.
[17] M. Meier, S. Karg, W. Riess, Light-emitting diodes based on poly-p-phenylene-vinylene: II. Impedance spectroscopy, Journal of Applied Physics, 82 (1997) 1961-1966.
[18] G. Dennler, C. Lungenschmied, N.S. Sariciftci, R. Schwodiauer, S. Bauer, H. Reiss, Unusual Electromechanical Effects in Organic Semiconductor Schottky Contacts: Between Piezoelectricity and Electrostriction, Applied Physics Letters, 87 (2005) 163501.
[19] M. Li, A. Patra, Y. Sheynin, M. Bendikov, Hexyl-Derivatized Poly(3,4-ethylenedioxyselenophene): Novel Highly Stable Organic Electrochromic Material with High Contrast Ratio, High Coloration Efficiency, and Low-Switching Voltage, Adv. Mater., 21 (2009) 1707-1711.
[20] G. Garcia-Belmonte, P.P. Boix, J. Bisquert, M. Sessolo, H.J. Bolink, Simultaneous determination of carrier lifetime and electron density-of-states in P3HT:PCBM organic solar cells under illumination by impedance spectroscopy, Solar Energy Materials and Solar Cells, 94 (2010) 366-375.
[21] G. Juska, K. Genevicius, R. Osterbacka, K. Arlauskas, T. Kreouzis, D.D.C. Bradley, H. Stubb, Initial transport of photogenerated charge carriers in pi-conjugated polymers, Phys. Rev. B, 67 (2003) 081201.
[22] C.-m. Kang, S. Kim, Y. Hong, C. Lee, Frequency analysis on poly(3-hexylthiopene) rectifier using impedance spectroscopy, Thin Solid Films, 518 (2009) 889–892.
[23] E.J. Meijer, A.V.G. Mangnus, B.H. Huisman, G.W. t Hooft, D.M. de Leeuw, T.M. Klapwijk, Photoimpedance spectroscopy of poly(3-hexyl thiophene) metal-insulator-semiconductor diodes, Synth. Met., 142 (2004) 53-56.

[24] J. Bisquert, G. Garcia-Belmonte, A. Munar, M. Sessolo, A. Soriano, H.J. Bolink, Band unpinning and photovoltaic model for P3HT:PCBM organic bulk heterojunctions under illumination, Chem. Phys. Lett., 465 (2008) 57-62.
[25] H.-F. Meng, T.-M. Hong, Deep defect levels and exciton dissociation in conjugated polymers, Physica B: Condensed Matter, 304 (2001) 119-136.
[26] F.C. Krebs, K. Norrman, Lifetimes of organic photovoltaics: Using TOF-SIMS and 18O 2 isotopic labelling to characterise chemical degradation mechanisms, Solar Energy Materials and Solar Cells, 90 (2006) 213-227.
[27] K. Norrman, N.B. Larsen, F.C. Krebs, Lifetimes of organic photovoltaics: Combining chemical and physical characterisation techniques to study degradation mechanisms, Solar Energy Materials and Solar Cells, 90 (2006) 2793-2814.
[28] L. Luer, H.J. Egelhaaf, D. Oelkrug, G. Cerullo, G. Lanzani, B.H. Huisman, D. de Leeuw, Oxygen-induced quenching of photoexcited states in polythiophene films, Org. Electron., 5 (2004) 83-89.
[29] M.-Y. Chiu, U.S. Jeng, C.-H. Su, K.S. Liang, K.-H. Wei, Simultaneous Use of Small- and Wide-Angle X-ray Techniques to Analyze Nanometerscale Phase Separation in Polymer Heterojunction Solar Cells, Adv. Mater., 20 (2008) 2573-2578.
[30] X. Lei, F. Zhang, T. Song, B. Sun, p-type doping effect on the performance of organic-inorganic hybrid solar cells, Applied Physics Letters, 99 (2011) 233305.